Regional Dynamic Viscoelastic Properties of Porcine Sclera

Undergraduate Honors Thesis

Presented in Partial Fulfillment of the Requirements for Graduation with Honors Research Distinction in the Department of Biomedical Engineering at The Ohio State University

By
Jared Artz
May 2016

Advisor: Jun Liu, Ph.D.

Abstract

The biomechanical properties of the posterior sclera are thought to be important in glaucoma susceptibility. Assessment of the posterior sclera biomechanics is currently unavailable in vivo but methods are being developed to characterize the biomechanical properties of the anterior portion of the eye. The objective of this study was to characterize the regional dynamic viscoelastic properties of porcine sclera to examine possible correlation between anterior and posterior sclera. Scleral strips were excised from the temporal region of the anterior and posterior portions of 30 porcine eyes within 24 hours post-mortem. The scleral strips were tested using a Rheometrics Systems Analyzer II in a humidity chamber at approximately 25 °C. A cyclic strain was applied to the strips and the cyclic stress output was recorded. A ramp test was also conducted. The biomechanical properties of the anterior and posterior scleral showed significant differences with a complex modulus of 1.67±0.63 and 0.35±0.1 MPa ($p<0.001$), a secant modulus at 1% strain of 1.17±0.67 and 0.17±0.06 MPa ($p<0.001$), and a dynamic viscosity of 0.04±0.015 and 0.008±0.033 ($p<0.001$). The thickness was also significantly different between the anterior and posterior sclera (0.99 mm and 1.58 mm, $p<0.001$) There was no correlation in thickness ($p>0.25$) or any biomechanical properties between the anterior and posterior sclera ($p>0.82$). These results provide insight to an interesting regional variance of the biomechanical properties of scleral tissue, which is not necessary proportional in the same eye. Future work will investigate scleral tissue microstructure to understand the structural basis of the mechanical difference from anterior to posterior eye.

Acknowledgements

There are numerous people I would like to thank for their invaluable assistance on this project. Without their crucial support this project would not have been successful.

The first person deserving thanks is Dr. Jun Liu. Without her guidance, challenge, and support I wouldn't have learned, pushed, and grown the way I have through this project. I am grateful for her critiques and advice that has pushed me to ensure this project stays on track and achieves its goals. Without her support this project would not have been successful.

I would like to express my gratitude to Dr. Hugh Morris as well. He was instrumental in aiding my adjustment to working in a research laboratory. Without his guidance I would not have been able to learn the skills necessary to complete this project. I am extremely grateful for his time, energy, and guidance in the early stages of my research in Dr. Liu's lab.

Lastly, I would like to thank Eli Pavalotas and Keyton Clayson. Their support and encouragement was invaluable. I appreciated their willingness to assist and provide expertise and knowledge that I lacked. Through their assistance I was able to adequately explain the results of this study.

Table of Contents

List of Tables and Figures

Chapter 1: Introduction

Glaucoma is an association of optic neuropathies characterized by the continual degeneration of retinal ganglion cells. Those cells have their axon in the optic nerve and their cell body in the inner retina. Cupping, an appearance of the optic disc and visual loss, occurs due to degeneration of these central nervous system neurons [1].

Glaucoma affects approximately 70 million people worldwide, with 7 million being bilaterally blind [2]. It is the second leading cause of blindness in the world [3]. Cupping often occurs in late stages of glaucoma, resulting in a high possibility that people are unaware they have glaucoma [4, 5]. Earlier work suggests that 10% to 50% of the people with glaucoma don't know they have it [6, 7]. The 2 categories of glaucoma are open-angle and angle-closure. In the United States approximately 80% of the cases are open-angle [8].

The pathogenesis associated with glaucoma is complex and not fully understood, there are multiple risk factors that affect glaucoma susceptibility of the patient. Risk factors include older age, genetics, systemic or topical corticosteroid use, race, and high intraocular pressure (IOP). Among the major factors contributing to glaucoma occurrence intraocular pressure (IOP) has been related to retinal cell death and studied extensively [9]. IOP is regulated through the secretion of aqueous humor by the ciliary body and drainage through the trabecular network and the uveoscleral outflow pathway. In open angle glaucoma, often increased resistance to aqueous humor drainage through the trabecular network causes an increase in IOP. In close-angle glaucoma the drainage pathway is obstructed by the iris, causing an increase in IOP.

IOP can cause mechanical stress and strain on the structures of the eye, specifically the posterior lamina cribosa and adjacent tissue [10]. It is thought that the IOP related strain on the posterior portion of the eye may develop deformation and remodeling of the lamina cribosa. This

may cause consequent axonal damage and disrupt axonal transport. As a consequence, essential trophic factors are eliminated from retrograde delivery to the retinal ganglion cells [11, 12].

In early stage glaucoma, axonal transport disruption occurs and results in disorganization of microtubules and neurofilaments in the prelaminar and post laminar regions. These ultrastructural changes have been observed in postmortem human globes that have glaucoma [13]. However, it has been shown that patient risk for glaucoma can vary among patients with similar IOP or can occur in patients with relatively normal IOP levels. It is thought that the patients may have abnormally low cerebrospinal fluid pressure in the optic nerve subarachnoid space, consequently having a large pressure gradient across the lamina cribosa [14, 15]. It is thought that the scleral strength of a patient may resist deformation by IOP and aid in protecting the optic nerve head from damage during IOP elevations [16]. Therefore, an increased scleral strength may result in a lower risk for glaucoma and damage to the optic nerve head retinal ganglion cells [17].

Currently, it is impossible for the posterior scleral tissue strength to be determined in vivo. If a correlation was established between the anterior and posterior scleral tissue, it would be possible to establish a reasonable estimate for the posterior scleral tissue strength when an anterior strength of an eye was known. If a correlation exists, the susceptibility to glaucoma for a patient could be predicted by measuring the more accessible anterior sclera in the front of the eye.

Extensive testing has been carried out to determine mechanical properties of sclera [18] and it has been reported that the posterior sclera was more compliant than the anterior sclera [19]. However, it is unclear whether the properties of the anterior and posterior scleral are

correlated in the same eye. If such correlation exists, it would allow patients' posterior scleral tissue properties to be predicted by measuring the anterior scleral tissue properties.

It is unclear as to how the microstructure of the tissue contributes to its mechanical properties. It is thought that the collagen and proteoglycan content may have great influence on the properties of the scleral tissue [20, 27]. Biochemical analysis of collagen and proteoglycan content in the anterior and posterior sclera may thus explain the difference and potential correlation of the measured mechanical properties in the sclera.

1.1 Focus of Thesis

This project focuses on establishing a correlation between the anterior and posterior scleral tissue mechanical properties. The purpose of this project is to investigate whether the posterior scleral tissue mechanical properties can be estimated from a known anterior scleral tissue mechanical properties.

1.2 Significance of Research

The establishment of a correlation may allow clinicians to estimate the mechanical properties of posterior scleral tissue if the anterior scleral tissue is known. As methods to determine the anterior scleral tissue biomechanical properties in vivo are being developed, it may provide clinicians with a method for better predicting patient susceptibility to glaucoma.

1.3 Thesis Overview

This thesis has three successive chapters. Chapter 2 describes the tissue preparation and testing. Chapter 3 details the results from the mechanical analysis and includes a discussion of the effect of microstructure arrangement on biomechanical properties. The final chapter, chapter 4, contains the conclusion which presents the key contributions, future applications and directions of this research.

Chapter 2: Methods

2.1 Sample Preparation

Thirty porcine eyes (n = 30) were obtained from Delaware Meats (Delaware, OH) within 6 hours postmortem. One eye was tested from each pair. The eyes were stored in phosphate buffered saline at 4°C until dissection. The extraocular tissue was removed and the corneal button was excised. The intraocular contents were then removed. The scleral shell was placed upon a polymer globe and an anterior and posterior strip were excised from the scleral tissue along the supero-inferioral axis on the temporal side using parallel blade excision device. A representation of the scleral cutting position can be seen in Figure 2. Width and thickness measurements were determined by measuring three spots along each strip, each end and the middle as shown in Figure 1. The average of those values was used to determine the thickness and width of the tissue strip. Each strip was stored in phosphate buffered saline at 4°C until mechanical testing. All testing was conducted within 36 hours postmortem.

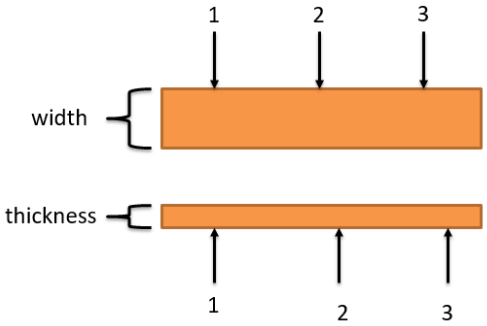

Figure 1: Illustration of measuring tissue strips.
Dimensions were taken at 1, 2, and 3 and averaged to provide thickness and width dimension for each strip.

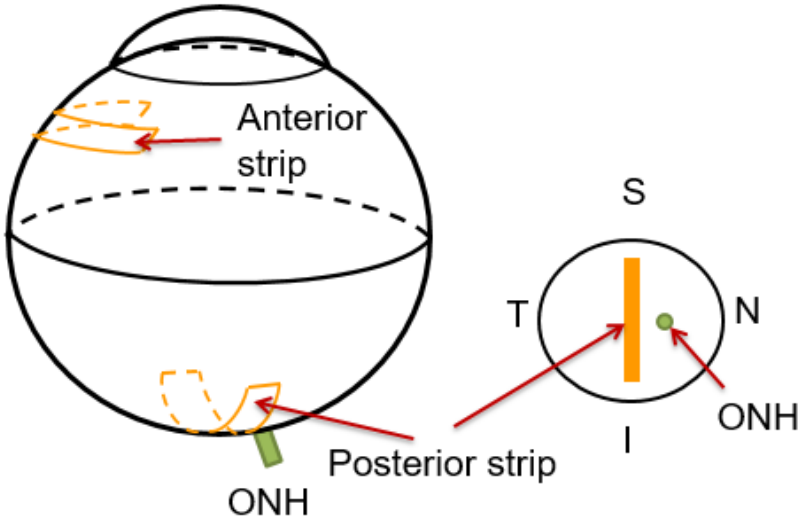

Figure 2: The anterior and posterior excision location of tissue on the globe

2.2 Mechanical Testing

Dynamic mechanical analysis (DMA) is a standard method to determine the viscoelastic properties of a material. [21, 22]. A minute, sinusoidal strain is applied to the sample and the resulting sinusoidal stress response is observed. A sample stress-strain curve is shown in Figure 3. Viscoelastic properties, such as complex modulus, dynamic viscosity, and tan(δ), can be calculated from the ratio of the stress to strain amplitudes along with the phase difference between the recorded stress response and the applied strain. The complex modulus, similar to Young's modulus but specific to dynamic loading, has two factors: the loss modulus and the storage modulus, the viscous and elastic factor respectively. The damping of the tissue is represented by tan(δ) and can be quantified by the ratio of loss modulus to storage modulus. The dynamic viscosity represents the internal damping of the tissue to dynamic force and is the ratio of the loss modulus to angular frequency.

A uniaxial testing system (Rheometrics Systems Analyzer III; TA Instruments; New Castle, DE) was used to mechanically strain the scleral tissue and record the load output. The

scleral strips were carefully aligned and secured in the clamps to ensure good grip and prevent slippage (Figure 4). The scleral strips were kept moist in a humidity chamber at approximately 23°C during testing. The scleral strips were preconditioned by varying the load from 1 g to 4-6 g for 5 cycles. The tissue was then equilibrated at 1.0 g for 5 minutes; after which it was preloaded to 2.0 g for 1 minute. A dynamic mechanical analysis (DMA) was conducted by applying a cyclic strain at 0.15% superimposed upon the preload. The cyclic load output was recorded. After DMA, the sample was equilibrated for 5 minutes at 1.0 g. A ramp test was conducted and a strain rate of 0.1%/s was applied up to 5% strain. The scleral strips were then stored at -80°C. An illustration of the testing protocol can be seen in Figure 5.

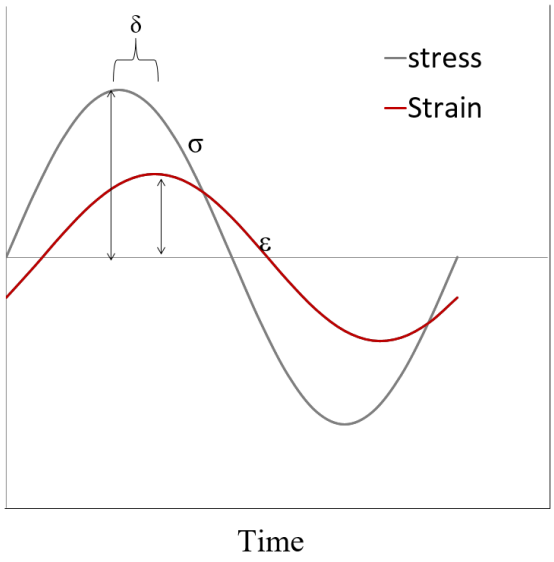

Figure 3: Stress-Strain curve during cyclic sinusoidal loading

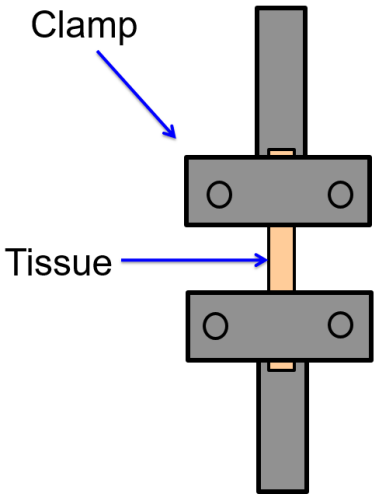

Figure 4: The mechanical loading positions of strips in the RSA III

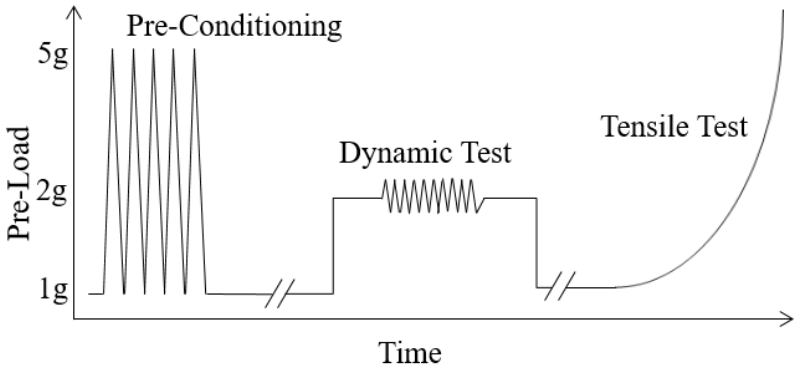

Figure 5: DMA and Tensile Testing Protocol

The stress and strain data obtained for each strip during the ramp test was fit to Fung's standard exponential model [23].

$$\sigma = A * (1 - e^{B\varepsilon})$$

The constants A and B were determined using a Levenberg-Marquardt least squares method. The initial elastic response of the tissue is represented by the magnitude of A*B and the slope of change in the tissue's tangent elastic modulus with increasing stress is represented by B.

Mechanical testing data was processed in MATLAB. Two MATLAB scripts that processed the data files was developed originally by Dr. Hugh Morris and modified for this project. They can be referenced in Appendix A: MATLAB Code. The first program, used for DMA analysis, requires the input of the sample cross-section dimensions, thickness and width previously gathered from a caliper. This program plots and fits the individual stress-strain curves and compile all the curves on individual plots. It also calculates and provides complex modulus, loss modulus, storage modulus, dynamic viscosity, and tan(δ). A sample output of the program can be seen in Figure 6 - 8. The second program, for ramp analysis, requires the input of the thickness and width dimensions of the sample. It plots and fits the individual stress strain curves and compiles all the curves on individual plots. It also calculates the secant modulus for each sample at strains of 1%, 2%, and 3% and the constants A and B. A sample output of the program can be seen in Figure 9 - 11.

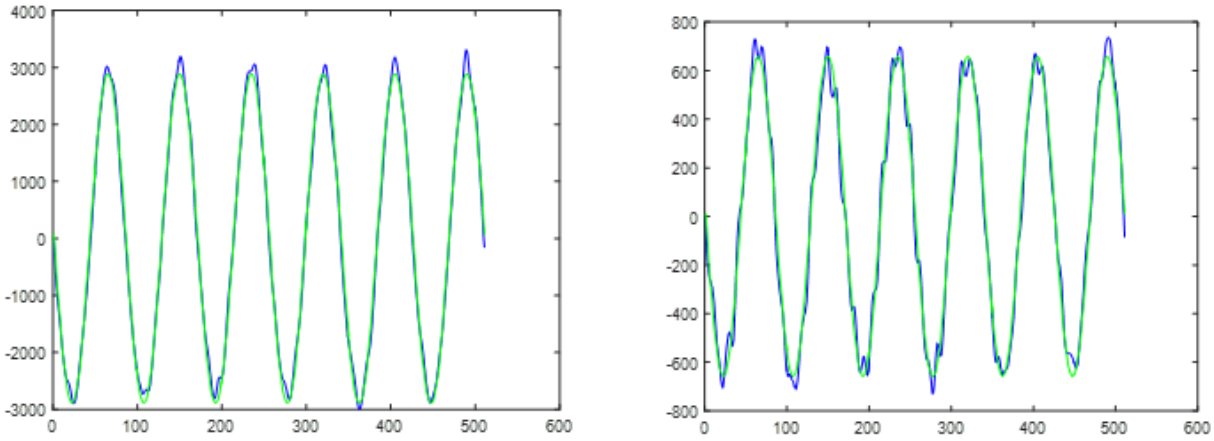

Figure 6: MATLAB plot of dynamic stress output of anterior (left) and posterior (right) strips from globe 3. The blue curve represents the stress output and the stress fit is represented by the green curve. The y-axis is the stress magnitude (Pa) and the x-axis is the successive data points.

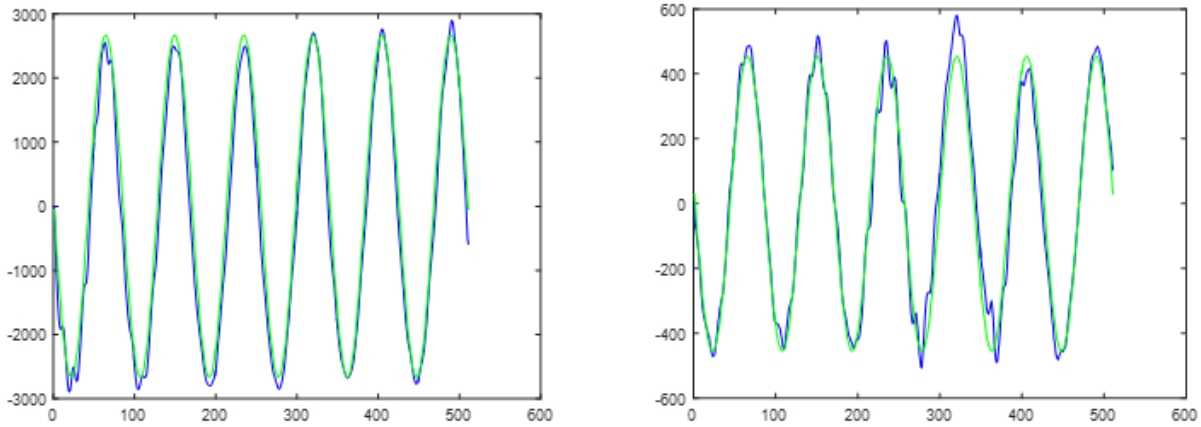

Figure 7: MATLAB plot of dynamic stress output of anterior (left) and posterior (right) strips from globe 28. The blue curve represents the stress output and the stress fit is represented by the green curve. The y-axis is the stress magnitude (Pa) and the x-axis is the successive data points.

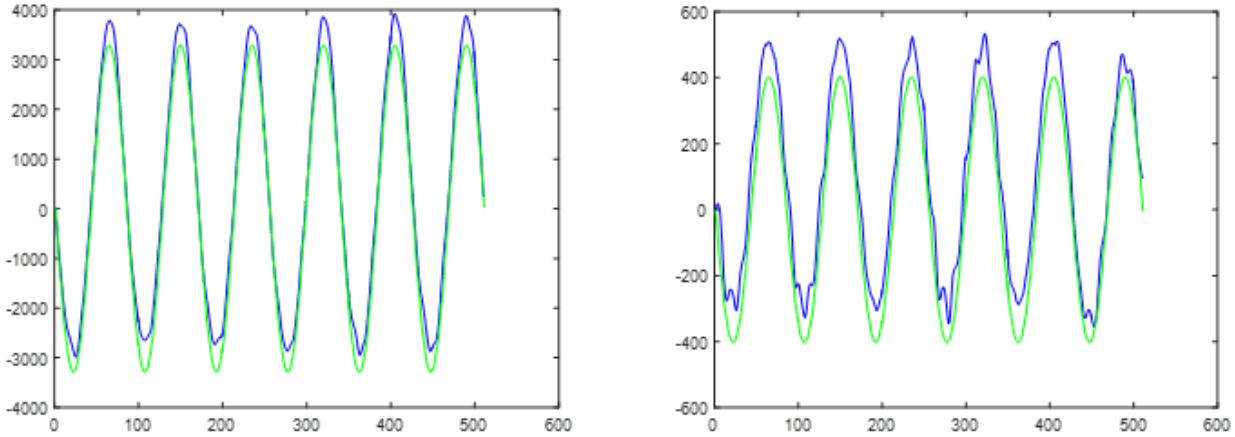

Figure 8: MATLAB plot of dynamic stress output of anterior (left) and posterior (right) strips from globe 30. The blue curve represents the stress output and the stress fit is represented by the green curve. The y-axis is the stress magnitude (Pa) and the x-axis is the successive data points.

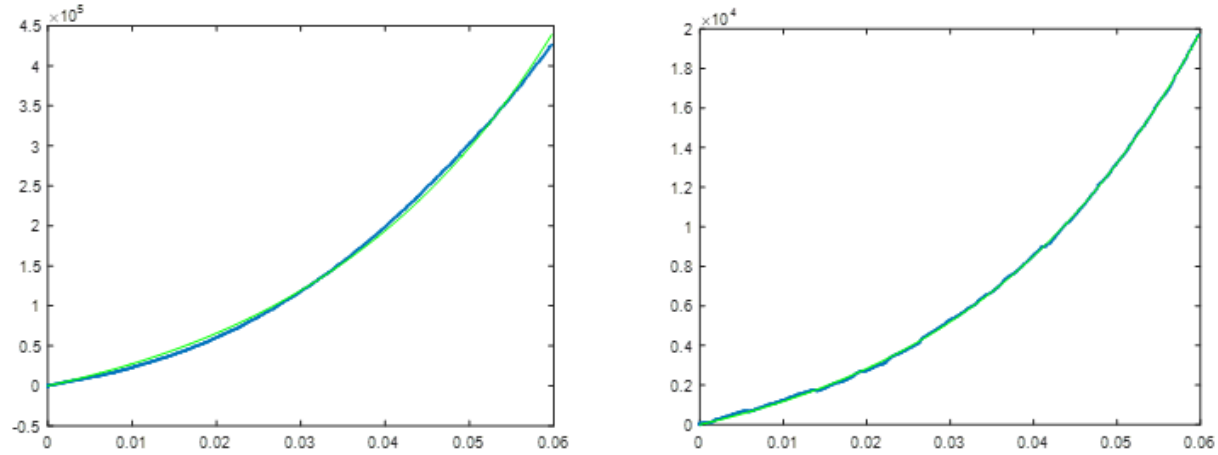

Figure 9: MATLAB plot of stress-strain output of anterior (left) and posterior (right) strips from globe 17. The blue curve represents the stress-strain output and the stress-strain fit is represented by the green curve. The y-axis is the stress magnitude (Pa) and the x-axis is strain magnitude.

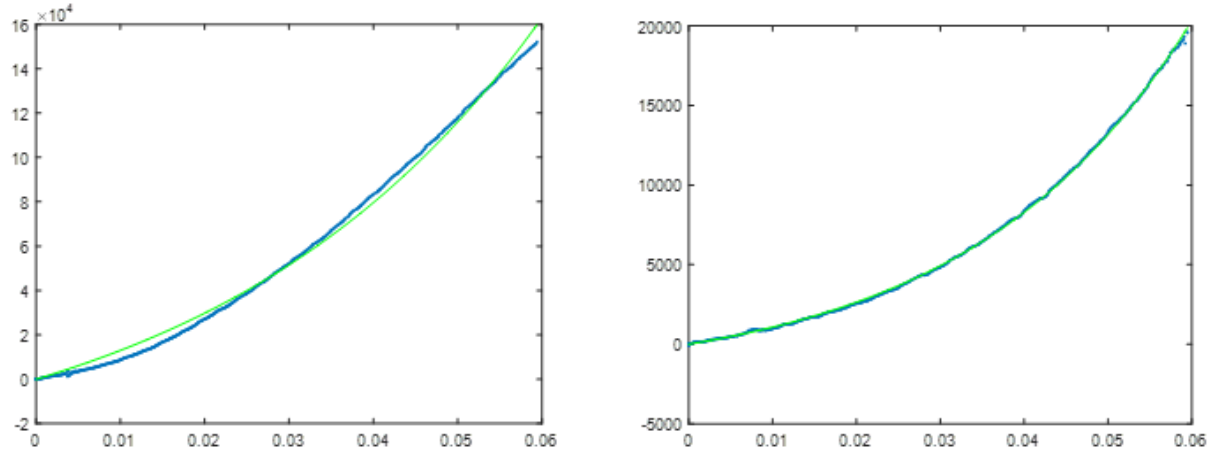

Figure 10: MATLAB plot of tensile stress output of anterior (left) and posterior (right) strips from globe 28. The blue curve represents the stress-strain output and the stress-strain fit is represented by the green curve. The y-axis is the stress magnitude (Pa) and the x-axis is strain magnitude.

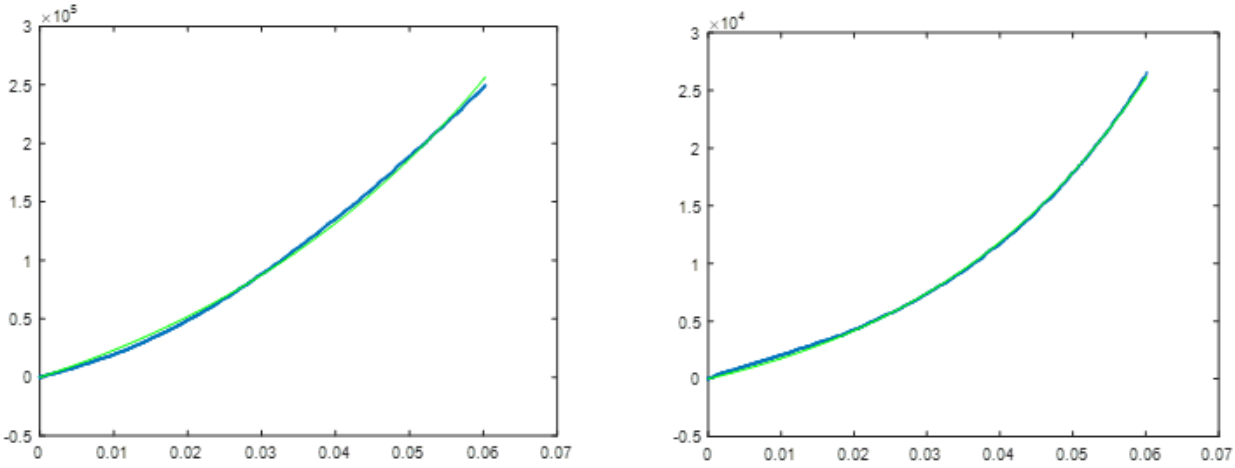

Figure 11: MATLAB plot of tensile stress output of anterior (left) and posterior (right) strips from globe 30. The blue curve represents the stress-strain output and the stress-strain fit is represented by the green curve. The y-axis is the stress magnitude (Pa) and the x-axis is strain magnitude.

2.3 Statistical Analysis

Statistical analysis was performed using JMP 13.1 software package (SAS Institute, Inc., Cary, NC). The comparison between the two scleral regions were performed on all eyes among multiple variables. The difference of the dynamic mechanical properties between the anterior and posterior strips were compared using paired student's t-tests. The properties from the tensile

ramp tests were compared using paired student's t-tests. Correlation coefficients between anterior and posterior sclera for biomechanical properties, including complex modulus, dynamic viscosity, and tan(δ), were calculated using Pearson's correlations.

Chapter 3: Results

For each globe the stress output was recorded and plotted for both the dynamic and quasi-static mechanical analyses. From those fitted plots the values were calculated as detailed in the methods. Sample plots that were produced from both of the analysis are shown in Figure 6. The major variables averages and standard deviations are displayed in Table 1.

Table 1: Mechanical Analysis Results

	Anterior		Posterior		p value
	Average	STD	Average	STD	
Width (mm)	3.29	0.21	3.28	0.22	0.941
Thickness (mm)	0.99	0.20	1.58	0.26	<0.001
Complex Modulus (MPa)	1.67	0.63	0.35	0.11	<0.001
Loss Modulus (MPa)	0.29	0.10	0.05	0.02	<0.001
Storage Modulus (MPa)	1.64	0.63	0.35	0.11	<0.001
Dynamic Viscosity	0.047	0.016	0.0082	0.0034	<0.001
Tangent Delta	0.18	0.03	0.15	0.03	<0.001
Secant Modulus at 3% (MPa)	1.80	1.00	0.24	0.09	<0.001

The dimensions of each strip were approximately the same, with respect to width, at 3.29 mm and 3.28 mm, anterior and posterior respectively, and differed in thickness with the posterior being on average 0.6 mm greater than the anterior ($p<0.001$). An increasing trend was observed in the posterior thickness as the experiments progressed, i.e., the eyes measured at a later week had a larger thickness ($R=0.8$, $p<0.001$, Fig 12).

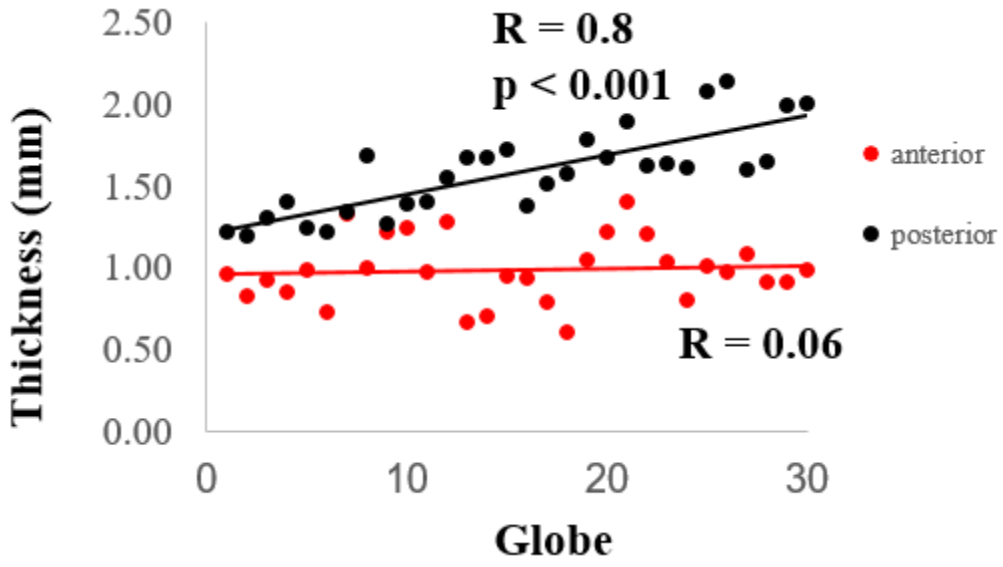

Figure 12: Comparison of thickness by globe.
The x-axis is the index of the eye sample as the experiment progressed from the first to fifth week; p value from paired t-test.

The average complex modulus was 1.67 ± 0.63 and 0.35 ± 0.11 MPa, for anterior and posterior sclera respectively. There was no significant correlation between the anterior and posterior properties as shown in Figure 13 (R= -0.25, p=0.1817). The anterior scleral complex modulus was higher than the corresponding posterior scleral complex modulus for every globe tested (Figure 14).

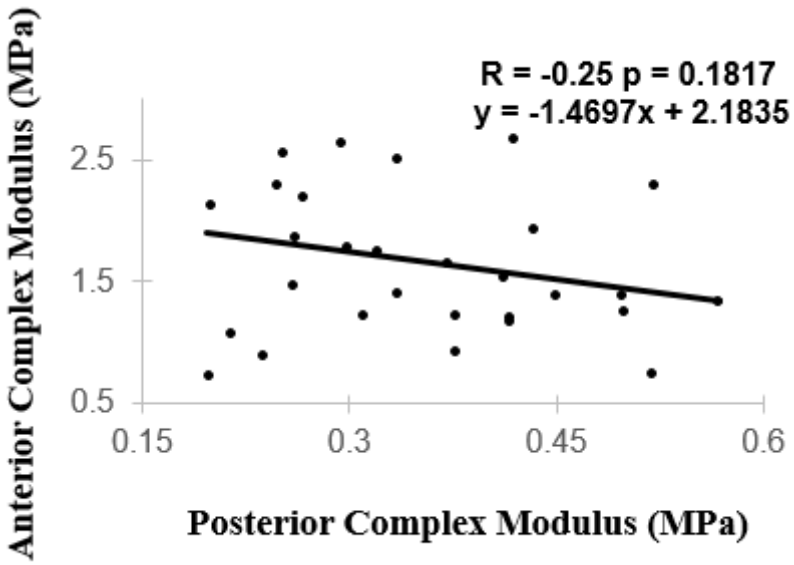

Figure 13: Correlation of anterior and posterior complex modulus.

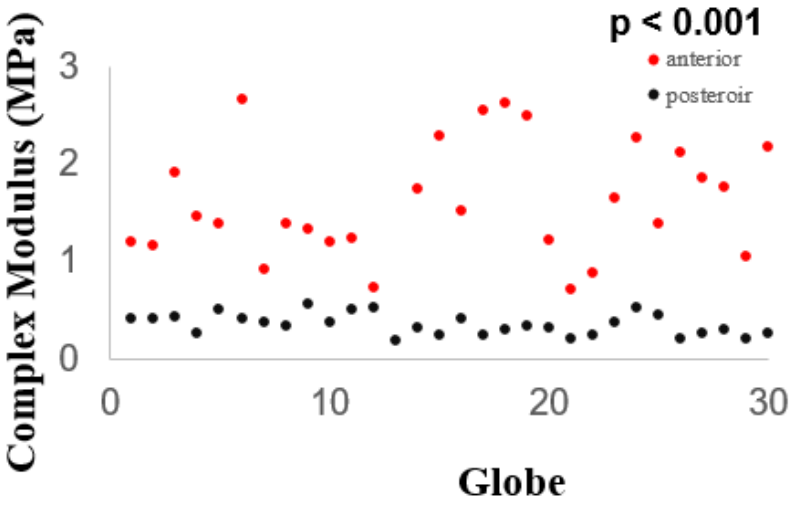

Figure 14: Comparison of complex modulus by globe.
The x-axis is the index of the eye sample as the experiment progressed from the first to fifth week; p-value from paired t-test.

The average secant modulus (3%) was 1.80 ± 0.98 and 0.24 ± 0.08, for anterior and posterior sclera respectively. There was no significant correlation observed between the anterior and posterior secant modulus as shown in Figure 15 (R=-0.004, p=0.9819). For all thirty globes, the

anterior sclera secant modulus was higher than the corresponding posterior secant modulus as shown in Figure 16 ($p < 0.001$).

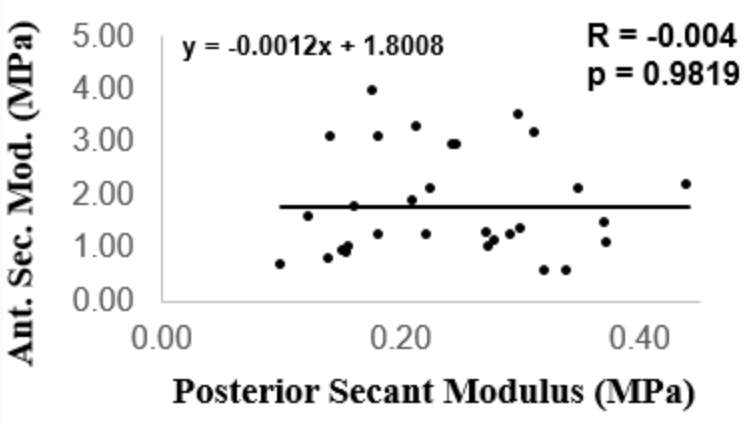

Figure 15: Correlation of anterior and posterior secant modulus (at 3% strain)

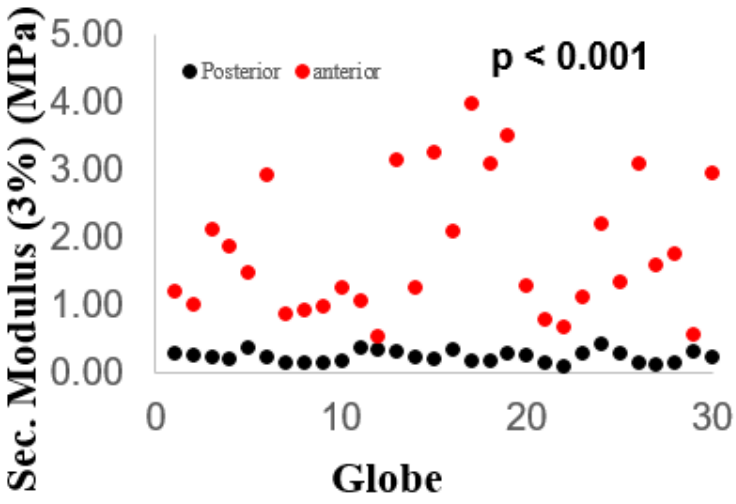

Figure 16: Comparison of secant modulus (at 3% strain) by globe.
The x-axis is the index of the eye sample as the experiment progressed from the first to fifth week; p-value from paired t-test.

The average dynamic viscosity, the ratio of loss modulus to angular frequency, was 0.0469 ± 0.0159 and 0.00826 ± 0.00337, for anterior and posterior sclera respectively. There was no

significant correlation observed between the anterior and posterior dynamic viscosity as shown in Figure 17 (R=-0.21, p=0.2727). For all thirty globes, the anterior sclera dynamic viscosity was higher than the corresponding posterior dynamic viscosity as shown in Figure 18 ($p < 0.001$).

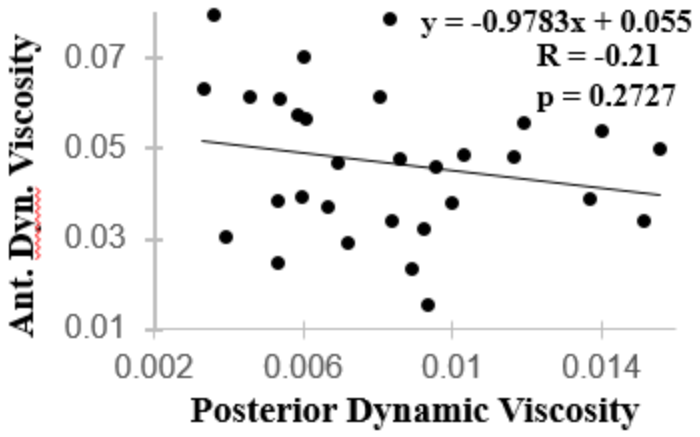

Figure 17: Correlation of anterior and posterior dynamic viscosity.

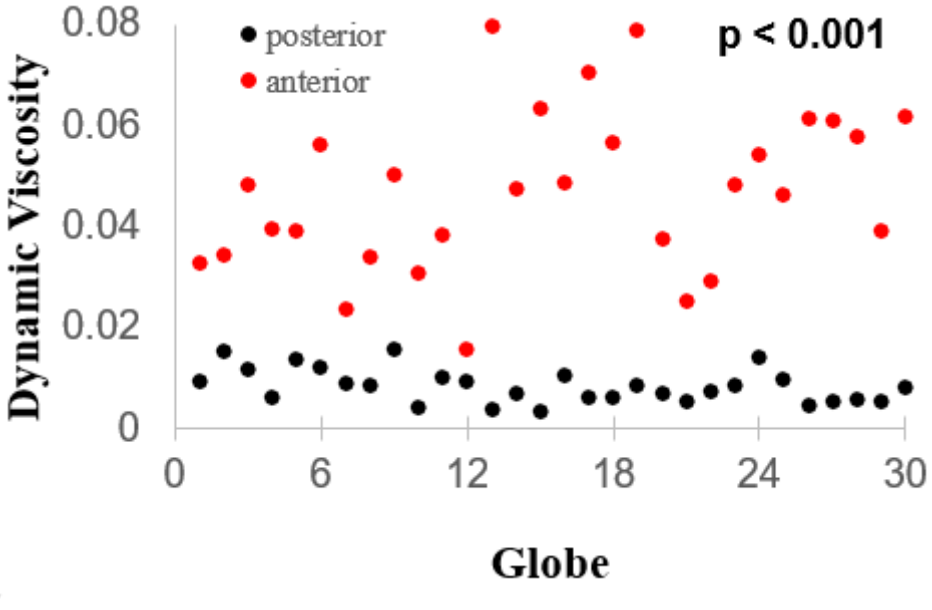

Figure 18: Comparison of dynamic viscosity by globe.
The x-axis is the index of the eye sample as the experiment progressed from the first to fifth week; p-value from paired t-test.

The tan(δ), the ratio between the loss and storage modulus, was 0.18 ± 0.03 and 0.15 ± 0.03, for anterior and posterior sclera, respectively. There was no significant correlation between the anterior and posterior values as seen in Figure 19 (R = 0.2, p=0.3173). The tangent delta appeared to overlap in magnitudes for the anterior sclera and the posterior sclera, yet overall the anterior was significantly greater than the posterior as seen in Figure 20 (p< 0.001).

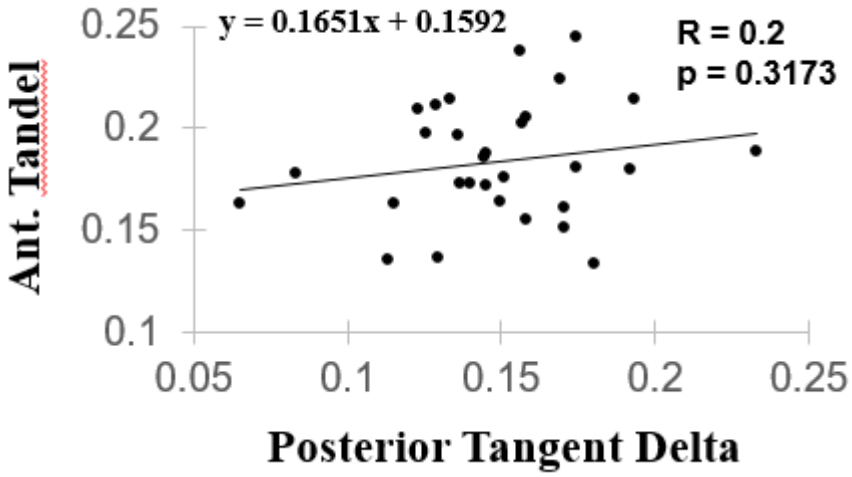

Figure 19: Correlation of anterior and posterior tangent delta.

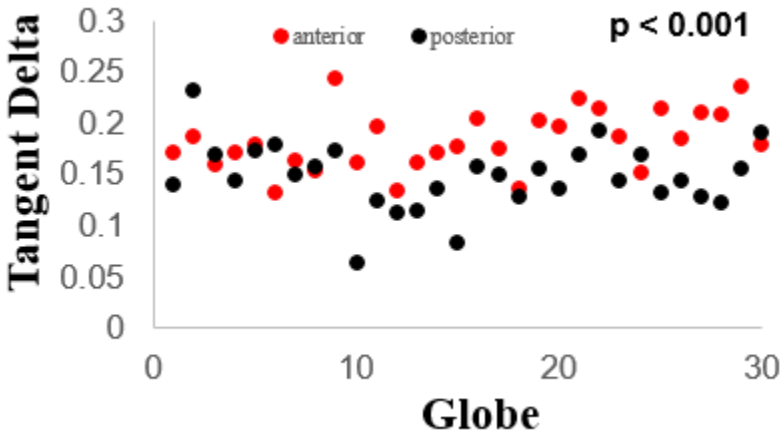

Figure 20: Comparison of tangent delta by globe.
The x-axis is the index of the eye sample as the experiment progressed from the first to fifth week; p-value from paired t-test.

Chapter 4: Discussion

An increasing posterior sclera thickness was observed in the tested eyes as the experiments progressed from week 1 to week 5 (Figure 12). Experimentation was conducted over 5 weeks and 6 eyes were tested each week on the same day. This trend coincided with the age trend in the animals. Globes #1 – 12 were from pigs that were 8 months old. Globes #13 – 24 were from pigs that were 6 months old. Globes #25 – 30 were from pigs that were 5½ months old. The posterior thickness vs globe index correlation did not exist within each week, when the animals were of the same age. (Figure 21). This appears to suggest that as a pig increases in age from 5 to 8 months, the thickness of the posterior sclera decreases. Pigs are often slaughtered at the age of 6 months for optimal meat quality, and this time may coincide with the maturity of the collagenous extracellular matrix in the posterior sclera. It appears that as the pig eye matures, the posterior scleral thickness decreases. Future studies are needed to further understand the posterior sclera thickness change during the animal's life span.

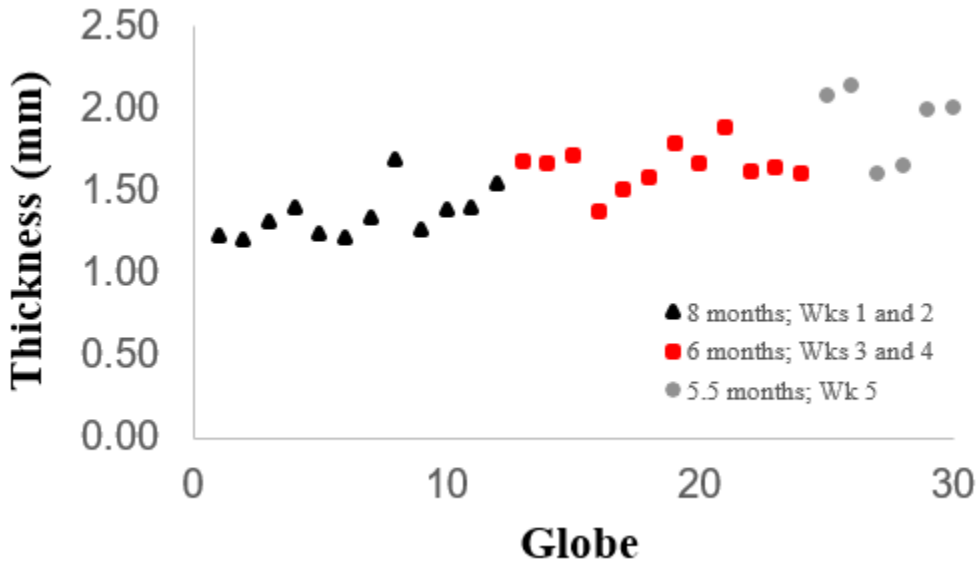

Figure 21: Thickness of Posterior Scleral Tissue by globe.
The x-axis is the index of the eye sample as the experiment progressed from the first to fifth week

Though globes #1 – 13 were from pigs around the same age, there is still a trend that increases with globe count. This may be explained by the difference in the pig's diets. Pigs that donated globes #1 – 6 were fed a high fat pizza scrap diet and the pigs that donated globes #7 – 12 were fed a normal diet and raised in poor conditions. Though the ages of the pigs were the same, the pigs that were fed a high fat diet may have developed faster and reached maturity faster than the pigs that were fed the normal diet and raised in poor conditions. As globes #1 – 6 were from pigs that may have reached maturity sooner than globes #7 – 12 the development would have slowed sooner and the thickness of the posterior scleral tissue would be less. A previous study on human donor eyes have shown an effect of age on the peripapillary scleral thickness with a decreasing thickness in older donors from 40 to 90+ years old [24].

The average complex modulus, a combination of the loss and storage modulus, was 1.67 ± 0.63 MPa and 0.35 ± 0.11 MPa, for the anterior and posterior sclera, respectively. The stiffer response of the anterior sclera in comparison to the posterior sclera could be influenced by collagen fibril size and arrangement, as well as the attachment of extraocular tissue. In the anterior sclera, the collagen fibrils are small to medium and compactly arranged. In contrast, the posterior sclera has medium to large collagen fibrils in a loose arrangement. This loose arrangement of the fibrils allows the tissue to be extended over a longer length with a lower force. The compact arrangement resists deformation and thus requires a larger force to extend the tissue [25]. The collagen fibrils in anterior region have highly circumferential alignment around the limbus. High circumferential alignment in the peripapillary sclera region was also shown due to the annulus collagen ring surrounding the optic nerve head. However, the dissected posterior strip was some distance away from the collagen annulus ring, and therefore the circumferential

arrangement was likely not as prominent. This alignment difference may result in the anterior tissue having a larger modulus than the posterior [26].

This observed increased modulus of the anterior region over the posterior region may serve a practical function that may be better understood with investigation of the extraocular tissue, age of tissue, and location of other tissues in the eye. The anterior sclera is close to the limbus, and the insertion point for extraocular muscles. The limbus is under high stress to maintain the shape of the corneal button, allowing proper focusing of light. This stress can be transferred to the anterior sclera. Additionally, the tendon fibers of extraocular muscles intermingle with the scleral fibers. This microstructure, where tendons intermingle, could have a stiffer response due to increased amount of strain resistant material. When the extraocular muscles act on the globe, the stress is imparted onto the sclera, where the tendons intermingle. This stress may condition the tissue to have increased extracellular matrix (ECM) and collagen compactness that may increase scleral stiffness. This increased scleral stiffness would be needed to resist the forces imparted by the extraocular muscles and the limbus.

The increased ECM in the anterior tissue may also be due to age. The scleral tissue originates in the posterior eye and moves forward to the limbus over time. More mature tissue, with ECM highly developed, is present in the anterior region and younger tissue, with freshly generated ECM, is present in the posterior region [27].

The average dynamic viscosity, a ratio between loss modulus and angular frequency, differed significantly between the anterior and posterior regions, 0.047 ± 0.016 and 0.0082 ± 0.0034 ($p<0.001$), respectively. Proteoglycan content and concentration varies over time and regionally in the scleral tissue. The proteoglycans may affect the arrangement and composition of the tissue microstructure and consequently the biomechanical properties. In the anterior region, three

primary proteoglycans, biglycan, decorin, and aggregan, decrease as the age of the patient increases. In the posterior region, biglycan and decorin decrease as the age of the patient increases whereas aggregan content is roughly constant. Aggregan distribution in the scleral tissue heavily favors the posterior region. Approximately 18% and 70% aggregan is distributed in the anterior and posterior regions, respectively. Aggregan binds water and increases water retention of the tissue when its distribution in a specific region increases. The decreased water retention of the anterior may decrease pliability and increase its viscosity as shown by the dynamic viscosity of 0.047. The posterior region, having a larger aggregan distribution, would see increased water retention which may increase pliability and decrease viscosity as shown by the dynamic viscosity of 0.0082 [28, 29].

Examining the tangent delta, a ratio between loss and storage modulus, may also be explained by aggregan distribution like dynamic viscosity. The tangent delta was 0.18 ± 0.03 and 0.15 ± 0.03, for anterior and posterior sclera respectively. The anterior region had a larger delta between initial strain and the stress response than the posterior region. This is due to the higher loss modulus, representing the viscous portion, of the anterior region than the posterior region. The decreased viscous portion of the posterior may be due to increased aggregan content when compared to the anterior.

The lack of a significant correlation in the complex modulus, dynamic viscosity, and tangent delta between the anterior and posterior scleral tissue suggests great variability in individual eye development and scleral structure between globes. The scleral variability is most likely due to variations in collagen fibril size and arrangement, age of tissue, and proteoglycan distribution and content. As there is no significant correlation between the scleral regions' biomechanical

properties, other methods will have to be investigated to potentially determine the posterior regional properties in-vivo.

Chapter 5: Conclusion

There is not a significant correlation between the biomechanical properties of the anterior and posterior scleral regions in porcine models. This set of data is moderate in scope, yet provides results suggesting that it is unlikely to predict the posterior scleral properties from known anterior scleral properties in-vivo. The difference between the regional scleral properties may be explained by microstructure arrangement and content, specifically collagen fibril size and arrangement and proteoglycan distribution.

For future work, the correlation between biomechanical properties and microstructure should be further investigated. Understanding the role of proteoglycans on the microstructure arrangement and indirectly on the biomechanical properties of the regional scleral tissue could provide novel methods to alter tissue strength. Analyzing proteoglycan content would provide further insight into studies where collagen content has been associated with biomechanical properties.

There exists a clinical need for a method that is able to obtain accurate in vivo measurements of the mechanical properties of the eye, including the posterior scleral tissue. Though mechanical properties are not significantly correlated between regions for scleral tissue, the investigation of mechanical properties and microstructure arrangement and content for regional scleral tissue may provide ways to predict and modify posterior scleral tissue properties.

References

1. Weinreb RN, Khaw PT. Primary open-angle glaucoma. Lancet. 2004; 363(9422):1711–1720. [PubMed: 15158634]
2. Quigley HA, Broman AT. The number of people with glaucoma worldwide in 2010 and 2020. Br J Ophthalmol. 2006; 90(3):262–267. [PubMed: 16488940]
3. Quigley HA. Neuronal death in glaucoma. Progress in Retinal and Eye Research. 1999;18:39–57. [PubMed: 20498]
4. Leite MT, Sakata LM, Medeiros FA. Managing glaucoma in developing countries. Arq Bras Oftalmol. 2011; 74(2):83–84. [PubMed: 21779659]
5. Rotchford AP, Kirwan JF, Muller MA, Johnson GJ, Roux P. Temba glaucoma study: a population-based cross-sectional survey in urban South Africa. Ophthalmology. 2003; 110(2):376–382. [PubMed: 12578784]
6. Hennis A, Wu SY, Nemesure B, Honkanen R, Leske MC. Barbados Eye Studies Group. Awareness of incident open-angle glaucoma in a population study: the Barbados Eye Studies. Ophthalmology. 2007; 114(10):1816–1821. [PubMed: 17698198]
7. Budenz DL, Barton K, Whiteside-de Vos J, et al. Tema Eye Survey Study Group. Prevalence of glaucoma in an urban West African population: the Tema Eye Survey. JAMA Ophthalmol. 2013; 131(5):651–658. [PubMed: 23538512]
8. Friedman DS, Wolfs RC, O'Colmain BJ, et al. Eye Diseases Prevalence Research Group. Prevalence of open-angle glaucoma among adults in the United States. Arch Ophthalmol. 2004; 122(4):532–538. [PubMed: 15078671]).
9. Allingham, R.R., Shields, M.B., 2005. Shields' Textbook of Glaucoma. Lippincott Williams & Wilkins, Philadelphia.
10. Quigley HA, Addicks EM, Green WR, Maumenee AE. Optic nerve damage in human glaucoma, II: the site of injury and susceptibility to damage. Arch Ophthalmol. 1981; 99(4):635–649. [PubMed: 6164357]
11. Fechtner RD, Weinreb RN. Mechanisms of optic nerve damage in primary open angle glaucoma. Surv Ophthalmol. 1994; 39(1):23–42. [PubMed: 7974188]
12. Burgoyne CF, Downs JC, Bellezza AJ, Suh JK, Hart RT. The optic nerve head as a biomechanical structure: a new paradigm for understanding the role of IOP-related stress and strain in the pathophysiology of glaucomatous optic nerve head damage. Prog Retin Eye Res. 2005; 24(1):39–73. [PubMed: 15555526]
13. Quigley HA, Addicks EM, Green WR, Maumenee AE. Optic nerve damage in human glaucoma, II: the site of injury and susceptibility to damage. Arch Ophthalmol. 1981; 99(4):635–649. [PubMed: 6164357]
14. Wang N, Xie X, Yang D, et al. Orbital cerebrospinal fluid space in glaucoma: the Beijing Intracranial and Intraocular Pressure (iCOP) study. Ophthalmology. 2012; 119(10):2065e1–2073e1. [PubMed: 22749084]
15. Ren R, Jonas JB, Tian G, et al. Cerebrospinal fluid pressure in glaucoma: a prospective study. Ophthalmology. 2010; 117(2):259–266. [PubMed: 19969367]
16. Eilaghi, A., et. al., (2010). Biaxial Mechanical Testing of Human Sclera. *Journal of Biomechanics, 43*, 1696-1701

17. Norman RE, Flanagan JG, Sigal IA, Rausch SMK, Tertinegg I, Ethier CR. Finite element modeling of the human sclera: Influence on optic nerve head biomechanics and connections with glaucoma. Experimental Eye Research. 2011;93:4–12. [Pubmed: 20883693]
18. Elsheikh, A., Geraghty, B., Alhasso, D., Knappett, J., Campanelli, M., & Rama, P. (2010). Regional variation in the biomechanical properties of the human sclera. *Experimental Eye Research*, 624-633.
19. Friberg, T.R., Lace, J.W., 1988. A comparison of the elastic properties of human choroid and sclera. Experimental Eye Research 47, 429-436.
20. Palko JR, Iwabe S, Pan X, Agarwal G, Kom´aromy AM, Liu J.Biomechanical properties and correlation with collagen solubility profile in the posterior sclera of canine eyes with an ADAMTS10 mutation. *Invest Ophthalmol Vis Sci*. 2013;54:2685– 2695
21. Ferry J. Viscoelastic Properties of Polymer. New York, NY: John Wiley & Sons; 1980.
22. Fung Y. Biomechanics: Mechanical Properties of Living Tissues. New York, NY: Springer; 1993
23. Mihai C, Iscru DF, Druhan LJ, Elton TS, Agarwal G. Discoidin domain receptor 2 inhibits fibrillogenesis of collagen type 1. J Mol Biol. 2006;361:864–876
24. Coudrillier, Baptiste, Jing Tian, Stephen Alexander, Kristin M. Myers, Harry A. Quigley, and Thao D. Nguyen. "Biomechanics of the Human Posterior Sclera: Age- and Glaucoma-Related Changes Measured Using Inflation Testing." *Investigative Opthalmology & Visual Science Invest. Ophthalmol. Vis. Sci.* 53.4 (2012): 1714. Web.
25. Curtin, Brian J. "Physiopathologic aspects of scleral stress-strain."*Transactions of the American Ophthalmological Society* 67 (1969): 417.
26. Girard, Michaël JA, et al. "Quantitative mapping of scleral fiber orientation in normal rat eyes." *Investigative ophthalmology & visual science* 52.13 (2011): 9684-9693.
27. Watson, Peter G., and Robert D. Young. "Scleral structure, organisation and disease. A review." *Experimental eye research* 78.3 (2004): 609-623.
28. Muir H. Proteoglycans as organizers of the intercellular matrix. Seventeenth CIBA Medical Lecture. *Biochem Soc Trans.* 1982;11: 613–622.
29. Rada, Jody A., et al. "Proteoglycan composition in the human sclera during growth and aging." *Investigative ophthalmology & visual science* 41.7 (2000): 1639-1648.

Appendix A: MATLAB Code

DMAanalysis_v2_temp.m

```
function
[ss0,sn0,Stress,Stressfit,Strainfit,Del,tanDel,E,Estor,Eloss,DynVis,filenames] =
DMAanalysis_v2_temp(SampParams)

%SampParams is a 2*X array of widths and lengths in units of meters

%unit conversion
mmHgToPa = 133.322;
Ntog = 1000/9.81;

%define the parameters of the waveform
freq = 1; %in Hz
NumOfCyc = 16;
IgnoreCyc = 10;
afreq = 2*pi*freq;

%define the folders
MstrFolder = 'C:\Users\Jared\Documents\2015-2016\Research\RSA Data\Posterior DMA\';
MechDataFolder ='';
NumOfHeaderRows = 2;
%Define the smoothing window for the stress data (needed for RSA)
smoothing_window = 3;

%get the dynamic test data
tempfolder = [MstrFolder MechDataFolder];
filefilter = [tempfolder '.txt'];
filenames = uigetfile(filefilter,'MultiSelect','on');
[~,sf] = size(filenames);

%get the dynamic test data
for i= 1:sf
    data = dlmread([tempfolder filenames{i}],'\t',NumOfHeaderRows,0);
    t = data(:,1); %time in seconds
    tstp = data(3,1)-data(2,1); %in secs
    [sd,~] = size(data);
    PtsPerCyc = round(sd/NumOfCyc);

    %get the rest of the data ignoring the first two cycles
    data = data(PtsPerCyc*IgnoreCyc+1:end,:);
    [sd,~] = size(data);
    t = data(:,1); %time in seconds
    Force(:,i) = data(:,4); %N
    %Stress(:,i) = data(:,2)/10;
    Stress(:,i) =Force(:,i)./(SampParams(i,1)*SampParams(i,2)); %in MPa
    for ii=1+smoothing_window:sd-smoothing_window
        Stress(ii,i) = mean(Stress(ii-smoothing_window:ii+smoothing_window,i));
    end
    Stress(:,i) = Stress(:,i)-Stress(1,i);
    ss0(1,i) = max(Stress(:,i));
    Strain(:,i) = data(:,3);
    sn0(1,i) = max(Strain(:,i));
    disp(:,i) = data(:,5);  %mm

    %Performing non-linear fit to the sine data
    model_eqn=@(A,t) A(1)*cos(afreq.*t+A(2));
    %Initial Guess of A
```

```
    A0(1)=ss0(1,i);
    A0(2)=0.1;
    %Options for the solver
    options=statset('FunValCheck','off');
    %Non-linear fit solver
    [Stressfit(:,i),rss,Jss,covss,msess]=nlinfit(t,Stress(:,i),model_eqn,A0,options);
    A0(1)=sn0(1,i);
    [Strainfit(:,i),rsn,Jsn,covsn,msesn]=nlinfit(t,Strain(:,i),model_eqn,A0,options);

    figure
    plot(Stress(:,i),'b-')
    hold on
    plot(Stressfit(1,i)*cos(afreq.*t+Stressfit(2,i)),'g');

%     figure
%     plot(Strain(:,i),'b-')
%     hold on
%     plot(Strainfit(1,i)*cos(afreq.*t+Strainfit(2,i)),'g');

    Del(:,i) = abs(Strainfit(2,i)-Stressfit(2,i));
    tanDel(:,i) = tan(Del(:,i));

    E(:,i)=Stressfit(1,i)/Strainfit(1,i)./1e6; %complex modulus in MPa
    Estor(:,i) = E(:,i)*cos(Del(:,i));
    Eloss(:,i) = E(:,i)*sin(Del(:,i));
    tand(:,i) = Eloss(:,i)/Estor(:,i);
    DynVis(:,i) = Eloss(:,i)/afreq;

    disp(['Processed file ' num2str(i) ' of ' num2str(sf)]);
end

return
```

RampTestanalysis_v2.m

```
function [Sec,Strain,Stress,A,B,AB] = RampTestanalysis_v2(SampParams)
%unit conversion
mmHgToPa = 133.322;
Ntog = 1000/9.81;
ForceCalCorr = 1; %2.6

%define the folders
MstrFolder = 'C:\Users\Jared\Documents\2015-2016\Research\RSA Data\Anterior Ramp\';
MechDataFolder ='';
NumOfHeaderRows = 2;
%Define the smoothing window for the stress data (needed for RSA)
smoothing_window = 3;

%get the dynamic test data
tempfolder = [MstrFolder MechDataFolder];
filefilter = [tempfolder '.txt'];
filenames = uigetfile(filefilter,'MultiSelect','on');
sf = max(size(filenames));

for i=1:sf
    data = dlmread([tempfolder filenames{i}],'\t',NumOfHeaderRows,0);
    t = data(:,1); %time in seconds
    tstp = data(3,1)-data(2,1); %in secs
    [sd] = max(size(data));
    Strain(:,i) = data(:,3);
```

```
    sn0 = max(Strain(:,i));
    Force(:,i) = data(:,7)./ForceCalCorr; %N
    %response = inputdlg('What is the length in mm?');
    len=SampParams(i,1); %str2num(char(response));
    %response = inputdlg('What is the width in mm?');
    wid=SampParams(i,2); %str2num(char(response));
    Stress(:,i) = Force(:,i)./(len*wid); %in MPa
    for ii=1+smoothing_window:sd-smoothing_window
        Stress(ii,i) = mean(Stress(ii-smoothing_window:ii+smoothing_window,i));
    end
    ss0 = find(Stress(:,i)==max(Stress(:,i)));
    StressRamp = cat(1,0,Stress(1:end,i));
    StrainRamp = cat(1,0,Strain(1:end,i));

    %find the secant modulus
    ind1 = min(find(StrainRamp>0.01)); Sec(i,1) = (StressRamp(ind1).*(100/1))./1E6;
    ind2 = min(find(StrainRamp>0.02)); Sec(i,2) = (StressRamp(ind2).*(100/2))./1E6;
    ind3 = min(find(StrainRamp>0.03)); Sec(i,3) = (StressRamp(ind3).*(100/3))./1E6;
    %ind4 = min(find(StrainRamp>0.04)); Sec(i,4) = StressRamp(ind4).*(100/4);
    %ind5 = min(find(StrainRamp>0.05)); Sec(i,5) = StressRamp(ind5).*(100/5);
    %ind6 = min(find(StrainRamp>0.06)); Sec(i,6) = StressRamp(ind6).*(100/6);


    %Performing non-linear fit to the sine data
    model_eqn=@(A,t) (A(1)*(exp(A(2)*StrainRamp)-1));
    %Initial Guess of A
    A0(1)=0.02;
    A0(2)=20;
    %Options for the solver
    options=statset('FunValCheck','off');
    %Non-linear fit solver
    [Stressfit,rss,Jss,covss,msess]=nlinfit(t,StressRamp,model_eqn,A0,options);

    A(:,i) = Stressfit(1);
    B(:,i) = Stressfit(2);
    AB(:,i) = Stressfit(1)*Stressfit(2);

    figure
    plot(StrainRamp,StressRamp,'.')
    hold on
    plot(StrainRamp, (A(:,i)*(exp(B(:,i)*StrainRamp)-1)),'g')
    disp(['Processed file ' num2str(i) ' of ' num2str(sf)])
end

return
```

Appendix B: RSA III Procedure

Cutting Protocol

Prepared by Jared Artz

1 November 2015

Bevis Hall 320

1. Remove extraocular tissue from the globe so that there is no tissue attached to the scleral tissue
2. Make a cut on the edge of cornea, excise the corneal button
3. Remove the intraocular contents (vitreous humor, lense, etc.)
4. Fix the scleral shell upon a polymer globe
5. Using parallel blade excision cut anterior strip circumferentially 1 mm past the limbus
6. Using parallel blade excision cut poster strip 2 mm from the optic nerve head along the supero-inferioral axis on the temporal side
7. Measurement of dimensions
    - Width
        - Measure at the bottom, middle, and top of strip with digital calipers
        - Average values to obtain width
    - Thickness
        - Measure at the bottom, middle, and top of strip with digital calipers
        - Average values to obtain thickness
8. Storage
    - Place in PBS and store in fridge (4degC) until mechanical testing.

Tensile Testing Protocol

Prepared by Jared Artz based on protocol for corneal tissue by Marty Spang

1 November 2015

Location: CBEC

9. Turn on the pressure gauges to allow the machine to be pressurized
10. Turn machine on in the lower back left-hand corner
11. Start TA Orchestrator on the desktop computer
12. Remove clamps from box
    - Place long clamp on bottom
    - Place short clamp on top
13. Load tissue
    - Insert the scleral tissue into the clamps.
        - Line up with the vertical markings on clamps to ensure it is in center of clamps.
    - Leave extra scleral tissue on outside of clamps.
14. Hydration of Tissue
    - Set up humidifier to put constant stream of moisture directly onto the tissue strip
15. Enter TA Orchestrator and select Control Tab
    - Click on gap control panel
    - Click turn on motor button
16. Precondition the Tissue
    - Under gap control panel start at 0 g of force
    - Increase distance of clamps until force of 4-6 g is read
    - Decrease distance of clamps until force of 1 g is read
    - Repeat for 5 cycles
17. Set up DMA Test
    - Go to control tab
    - Select edit/start test
    - Name file
        - P_Sclera_1anterior_dma_pre2p0g_18Nov2015

- Edit geometry
    - Select edit geometry
    - Enter width and thickness, the length is read from the machine as the gap length
        - Check – ‘read test fixture gap’ to ensure length is read from machine
- Load test
    - Go to test setup button
        - Select stored test setups
        - Liu_DMA
            - Select Edit test and send wave
            - Double check settings
                - Should read - “0.0015*sin(6.283*t)” 350 points Per Zone with each of the 4 regions with 4 seconds.
- Increase length of clamps until preload of 2.0 g

18. Run DMA test
19. Equilibrate tissue
    - Bring load back down to 0.5 g through the gap control
    - Wait 5 minutes before continuing testing (export in this time)
20. Export
    - Use export tab to export the file as a .txt file
        - Enables it to be read by MATLAB
21. Set up Ramp Test
    - Go to control tab
    - Select edit/start test
    - Name file
        - P_Sclera_1anterior_ramp_0p1_pre0p5g_18Nov2015
    - Load test
        - Go to test setup button
            - Select stored test setups
                - Liu_Ramp
                    - Double check settings

        - Should read - 5% strain, 350 points per zone, 0.001 extension value, Hencky extension mode with 2 regions of 25 seconds each
    - Double check preload is 0.5 g. If not, adjust to preload of 0.5 g.
    - Run test
22. Run tensile ramp test
23. Export
    - Use export tab to export the file as a .txt file
        - Enables it to be read by MATLAB
24. Clean Up
    - Decrease gap length of clamps to < 5 mm.
    - Loosen screws
    - Remove tissue
    - Dry clamps
25. If more tissue samples need to be tested repeat steps 6 – 17. Otherwise proceed to 19.
26. Save files to portable flash drive
27. Clean Clamps
    - Dry with paper towel
    - Place back into box
28. Turn off machine
29. Close TA Orchestrator
30. Close off pressure valves
31. Leave and ensure door is locked